COBEM 2021 26th International Congress of Mechanical Engineering
ABCM Associação Brasileira de Engenharia e Ciências Mecânicas
November 22-26, 2021, Virtual Congress, Brazil

COB-2021-0825
REDUCED ORDER MODELING OF HIGHLY FLEXIBLE STRUCTURES

Arthur Longo Veronese
Flavio Luiz Cardoso Ribeiro
ITA - Instituto Tecnólogico de Aeronáutica - Praça Marechal Eduardo Gomes, 50 - Vila das Acacias, São José dos Campos - SP
alverons@ita.br
flaviocr@ita.br

Fernando José de Oliveira Moreira
EMBRAER - Av. Brg. Faria Lima, 2170 - Putim, São José dos Campos - SP
fernando.moreira@embraer.com.br

Abstract. *The search for more fuel-efficient aircraft is an everlasting goal of the aerospace industry. This ambition has led to some aircraft designs with a very high aspect ratio wing. For these cases, the linear theories that use the assumption of small displacements begin to get inaccurate, needing the use of a non-linear theory to calculate displacements. Commercial software can provide a very accurate calculation of these displacements but can be too computationally expensive to use for a real-time simulation. In this context, this paper brings a lumped mass strain-based non-linear structural model, and a reduced order model to further decrease the computational time of simulation while generating accurate displacements values. This work also studies the influence of non-linear terms on the structure dynamic aiming for high calculation performance. If successful, this structural model can also be used as input of more complex problems that include the whole aircraft, such as aeroelasticity and control systems. In the proposed model, the generalized coordinates are the element rotations connected with torsional springs enabling motion of in-plane bending. A modal decomposition and truncation model order reduction is applied to produce a non-linear reduced order model, where the generalized coordinates are the natural modes of the structure. The number of natural modes required to provide accurate displacement results depends on the complexity of applied external force, where simpler forces such as single concentrated forces require fewer modes and more complex forces such as multiple points and distributed forces require more modes. The reduced-order model was able to reduce up to 68% of computational time for a static deflection and 95% for a time simulation, while reducing the order of the model from n=20 to n=2, and still producing accurate deflections results compared to the literature even for large displacements. This work also concluded that the high order gyroscopic term that consumes most of the computational performance can be neglected, greatly contributing to these results.*

Keywords: *MOR, structures, non-linear, modeling.*

1. INTRODUCTION

Achieving higher efficiency aircraft is an everlasting goal for the aircraft industry. In order to produce lift for the aircraft to fly, one component of the aerodynamic force produced on the wing is drag, which correlates directly with fuel consumption, drag is divided into two major factors: parasite drag, related to the friction forces of the fluid's viscosity and induced drag related to the vorticity caused by a finite wing. One way to reduce the induced drag on an aircraft is to increase the aspect ratio of its wing. Aspect ratio is a design parameter of an aircraft defined by the square of the wingspan divided by the wing area, or the wingspan divided by the mean chord. However, increasing the aspect ratio indefinitely can lead to structural issues. Higher aspect ratios on a wing mean that the wingspan increases or the chord (width) decrease leading to slender wings, this can cause static failure or dynamic instability (i.e. flutter).

These issues are particularly important for airplanes with a very high aspect ratio (larger than 20). This is usually the case with High Altitude Long Endurance (HALE) aircraft, such as the NASA Helios. In these aircraft, large structural deflections lead to structural geometrically non-linearities. Linear models that are usually considered in aeroelastic modeling are not enough to describe the dynamics.

There are many studies which investigates the effects of structural non-linearities on the aeroelastic behavior of aircraft. Patil (1999) used a nonlinear beam model from Hodges (1990) to describe the flight dynamics of highly flexible airplanes. Brown (2003) modified the formulation, rewriting the equations in a strain-based form. Subsequently, the approach was improved by Shearer (2006) and Su (2008). Ribeiro *et al.* (2012) developed an interactive toolbox that implements the strain-based formulation. Rempel *et al.* (2020) used a multi-body model with strain calculated by the body's rotation to study the aeroelastic behavior of a cantilever wing with structural geometric non-linearity using Kane's Method.

Recently, a few studies treated the reduced-order modeling of highly flexible structure aeroelastic problems. Su and Cesnik (2014) used a strain-based geometrically non-linear model coupled with an aerodynamic model. By using modal decomposition, they created a simplified non-linear model that represents well the behavior of the full system and exhibited a very good convergenceof the results. However, the reduction of the computational time was not substantial, once the computational advantage of the new solution was sacrificed due to the requirement of recovering wing displacement and rotation from kinematics for every time step. Medeiros (2019) developed a reduced-order aeroelastic model including a neural network to fit the non-linear force. A significant reduction in simulation time while still having high accuracy was obtained.

Simulating the aircraft dynamics coupled with non-linear structural dynamics can be computationally expensive. In this context, a structural model order reduction is relevant to reduce the computational burden. This paper introduces a lumped mass non-linear model that mimics geometrically non-linear beams. The equations of motion are obtained using Hamiltonian mechanics. Then, a reduced-order model is obtained as follows: a modal decomposition is obtained from the linearized equations; the modal shapes are used as new generalized coordinates; the non-linear reduced-order equations are then obtained using Euler-Lagrange equations. This paper also studies the influence of non-linear gyroscopic terms of the structure dynamic aiming for high calculation performance.

The paper is organized as follows: firstly, the idea behind model order reduction is briefly recalled in Section 2. Secondly, the lumped-mass beam model is described in Section 3. Thirdly, the non-linear reduced order model is obtained in Section 4. Then, numerical results are presented in Section 5. Finally, conclusions and further work are discussed in Section 6.

2. MODEL ORDER REDUCTION

Being a dynamic study, the solution of the states needs to be found for each time step, the presence of a non-linear mass matrix with dimensions of the n elements used on the beam discretization can be very computationally expensive. In order to reduce computational processing time, this study uses a model order reduction (MOR) technique.

Model order reduction is about reducing the order of the problem at maximum until only essential information is left, at this point the simplification stops. Schilders *et al.* (2008). Figure 1 shows a graphic interpretation of model order reduction.

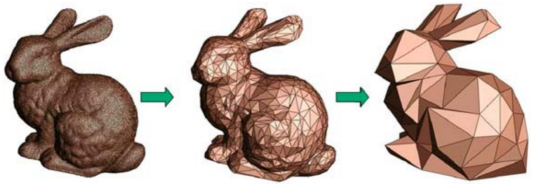

Figure 1. Graphic Illustration of Model Order Reduction. Schilders *et al.* (2008)

Dynamical systems can be represented by differential equations, such as:

$$\frac{d\boldsymbol{x}}{dt} = \boldsymbol{f}(\boldsymbol{x}, \boldsymbol{u}) \tag{1}$$

$$\boldsymbol{y} = \boldsymbol{g}(\boldsymbol{x}, \boldsymbol{u}) \tag{2}$$

in which **x** is the vector that contains the n state variables, **u** is the input vector and **y** is the output vector and the dynamic system can then be seen as an input-output system. The complexity of the system is defined proportionally by the number of n variables. Model order reduction has the objective of reducing the n state variables and at the same time preserving the input-output behavior of the model Schilders *et al.* (2008). In order to provide a good approximation, a few criteria should be satisfied: a small approximation error; preservation of properties of the original system, such as stability and passivity; and the fact that the reduction procedure should be computationally efficient Schilders *et al.* (2008). The reduced system is represented as:

$$\frac{d\hat{\boldsymbol{x}}}{dt} = \hat{\boldsymbol{f}}(\hat{\boldsymbol{x}}, \boldsymbol{u}) \tag{3}$$

$$\hat{\boldsymbol{y}} = \hat{\boldsymbol{g}}(\hat{\boldsymbol{x}}, \boldsymbol{u}) \tag{4}$$

where the dimension of $\hat{x}$ is much smaller than x, but $\hat{f}$ and $\hat{g}$ still accurately represents the input-output behavior of f and g. There are many other techniques in order to apply MOR. A more in-depth explanation of the other MOR methods is found at Schilders *et al.* (2008) and Sandberg (2019). Knowing these properties and the behavior of the system is up

to choose which case of MOR best applies to the system. For the case of this paper, it is important that the behavior of the reduced system at any time represents a good approximation of the original system. According to Sandberg (2019), for a successfully application of both methods, a good coordinate transformation and a suitable approximation order r is needed. In that case for the sake of simplicity, the Truncation method was chosen and its application will be further developed on Section 4.

3. LUMPED-MASS BEAM MODEL

The modeling of the beam is made through a lumped-model method. Subdividing into n elements, considering rigid body and concentrated mass at each element midpoint, the elements are connected by n torsional springs K_θ that are linked with the bending motion and n torsional springs K_ψ linked with the torsion motion. The motion of bending and torsion are initially uncoupled, but it is possible to couple these two motions by introducing a distance between the element center of mass and its neutral line.

The degrees of freedom are the absolute rotations of each beam. One thing to notice is that the rotations are measured relative to a global reference frame, not considering the previous element rotation, in order to produce independence between the elements. It is important to notice that large displacements and non-linear behavior are assumed only on the bending motion, whereas the torsion motion is assumed linear.

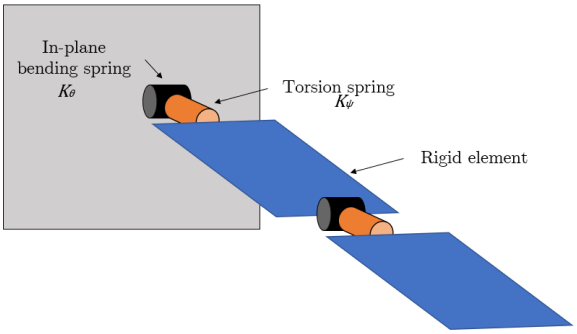

Figure 2. Example geometry beam model using n = 2 elements.

The vector that contains the generalized coordinates of the system is represented by $\boldsymbol{q}$, with dimension $2n$, where the first n elements represent the bending angles and the second half n elements represent the torsion angles.

$$\boldsymbol{q^T} = [q_1, q_2, \ldots, q_n, q_{n+1}, \ldots, q_{2n}] \tag{5}$$

The system stiffness is defined by $[K]$, a diagonal matrix, with dimensions $2n \times 2n$ containing the torsional stiffness of the bending and torsion springs respectively. While the mass of the system is defined by $[M]$, a square diagonal matrix with dimensions $3n \times 3n$ with the mass of each element instance repeated three times.

3.1 Element stiffness

Comparing to a continuous model of a cantilever beam, which has a bending stiffness described by EI, it is necessary to find the n values of K_θ that provides the same stiffness. A method was developed Rempel *et al.* (2020) for this purpose. It calculates a mean value of K_θ that is equal to all the elements and provides the same displacements of the linear model, and most important, proved that using the linear displacements to calculate the torsional springs stiffness is still accurate and can be used on non-linear models.

For this paper, a new method was developed, which calculates the values of each element stiffness K_θ, in order to better capture the behavior of the first elements close to the clamped geometrical condition and improve the approximation while using a low number of elements. With that in mind, the objective is to calculate the rotation (q), via Euler-Bernoulli Linear model, and the moment (M_z), obtained with the analytic beam moment distribution of each node with an applied unitary force on the beam tip. With every element rotation and moment, it is possible to calculate its stiffness using Hooke's Law:

$$K_{\theta,i} = \frac{M_{z,i}}{q_i} \qquad 1 \leq i \leq n \tag{6}$$

where $i \in \mathbb{N}$ with interval $1 \leq i \leq n$, represents the number of the element being calculated, with $i = 1$ the element on the wing root and $i = n$ on the tip. The same approach is used for calculating the stiffness of the torsion motion springs. For a continuous beam where its torsional stiffness is defined by GJ, it is necessary to compute the n values of spring stiffness K_ψ, but this process is simpler since the torsion motion was assumed linear.

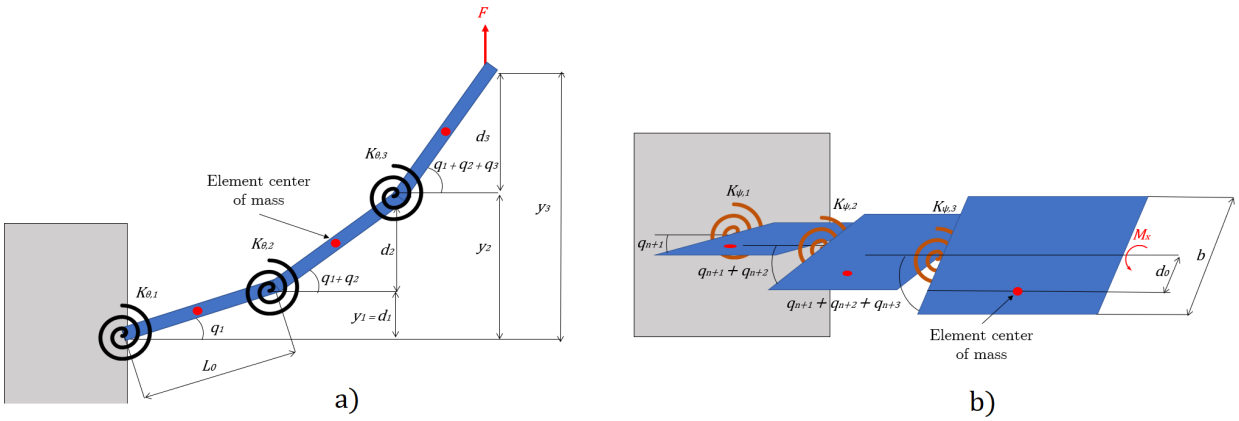

Figure 3. Example geometries of the deformed beam using n = 3 elements in a) bending and b) torsion motions.

Since the torque is constant through all the beam, and for the case where the cross-section is constant, all the values of K_ψ will be the same due to the angles being equal. This approximation is not able to include the effects of the clamping boundary condition of no rotation at $x = 0$, this means that the frequency calculated for torsion modes will be slightly more inaccurate. By applying Hooke's Law, the torsion stiffness is calculated:

$$K_{\psi,i} = \frac{M_{x,i}}{GJ} \qquad n+1 \leq i \leq 2n \tag{7}$$

The value of the first torsion stiffness element ($K_{\psi,1}$) is determined to be $2K_\psi$ to compute the geometrical restriction of the clamp that can not be obtained from the linear theory.

3.2 Equations of motion

The position of the element on the global frame is located at its center of mass. The element position has a contribution from the bending and torsion motion, they are calculated separately and summed afterward for each element. The coupling of torsion and bending motion appears on the non-linear mass matrix. It is possible to uncouple the torsion and bending motion by setting the element center of mass coincident to its centroid ($d_0 = 0$). The vector which contains the position of the elements in the global frame is given by

$$\boldsymbol{h(q)^T} = \left[\boldsymbol{x(q)^T}, \boldsymbol{y(q)^T}, \boldsymbol{z(q)^T}\right] , \tag{8}$$

where $\boldsymbol{x(q)} = [x_1(q), x_2(q), \ldots, x_n(q)]$, $\boldsymbol{y(q)} = [y_1(q), y_2(q), \ldots, y_n(q)]$ and $\boldsymbol{z(q)} = [z_1(q), z_2(q), \ldots, z_n(q)]$.

$$\begin{aligned}
x_{b,i}(q) &= x_{b,i-1} + L_0\left[cos\left(\sum_{j=1}^{i-1} q_j\right) + \frac{1}{2}cos\left(\sum_{j=1}^{i} q_j\right)\right] && 1 \leq i \leq n \\
y_{b,i}(q) &= y_{b,i-1} + L_0\left[sin\left(\sum_{j=1}^{i-1} q_j\right) + \frac{1}{2}sin\left(\sum_{j=1}^{i} q_j\right)\right] && 1 \leq i \leq n \\
z_{b,i}(q) &= 0 && 1 \leq i \leq n
\end{aligned} \tag{9}$$

and

$$\begin{aligned}
x_{t,i}(q) &= d_0 sin\left(\sum_{j=n+1}^{2i} q_j\right) sin\left(\sum_{j=n+1}^{2i} q_j\right) && 1 \leq i \leq n \\
y_{t,i}(q) &= d_0 cos\left(\sum_{j=n+1}^{2i} q_j\right) sin\left(\sum_{j=n+1}^{2i} q_j\right) && 1 \leq i \leq n \\
z_{t,i}(q) &= d_0 cos\left(\sum_{j=n+1}^{2i} q_j\right) && 1 \leq i \leq n
\end{aligned} \tag{10}$$

The motion of the system is obtained using Energy-based methods. The energy of the system is composed by kinetic energy from the movement of the elements, and the elastic potential energy stored on the spring elements of the system. The Lagrangian of the system is defined by

$$L = \frac{1}{2}\dot{\boldsymbol{q}}^{\boldsymbol{T}}[M_m(q)]\dot{\boldsymbol{q}} - \frac{1}{2}\boldsymbol{q}^{\boldsymbol{T}}[K]\boldsymbol{q} \tag{11}$$

where

$$[M_m(q)] = J_{h,q}^T[M]J_{h,q} \tag{12}$$

By applying Hamilton's Equations, the equations of motion are:

$$\frac{dq}{dt} = [M_m(q)]^{-1}\boldsymbol{p} \tag{13}$$

$$\frac{dp}{dt} = -[K]\boldsymbol{q} - \frac{\partial}{\partial \boldsymbol{q}}\left(\boldsymbol{p}^{\boldsymbol{T}}[M_m(q)]^{-1}\boldsymbol{p}\right) - C\dot{\boldsymbol{q}} + F[B(q)] \tag{14}$$

where

$$[B(q)] = J_{r,1,q}^T\left[-sin\left(\sum_{i=1}^{n} q_i\right) \quad , \quad cos\left(\sum_{i=1}^{n} q_i\right) \quad , \quad 0\right]^T \tag{15}$$

and

$$\boldsymbol{r_1} = \left[x(q) = \sum_{i=1}^{n} x_i + L_0 cos(q_i) \quad , \quad y(q) = \sum_{i=1}^{n} x_i + L_0 sin(q_i), \quad z(q) = 0\right]^T \tag{16}$$

3.3 Computation of gyroscopic term

The term $\frac{\partial}{\partial \boldsymbol{q}}\left(\boldsymbol{p}^{\boldsymbol{T}}[M_m(q)]^{-1}\boldsymbol{p}\right)$ of Equation (14) can be very computational expensive. The differentiation means that the matrix inversion needs to be done with symbolical math for its further calculation. To avoid that, two techniques were used to create the gradient without symbolical math: one exact solution using automated differentiation with the aid of the external *Matlab* package Adigator Patterson *et al.* (2013), and another using a numerical differentiation described by

$$\frac{\partial f}{\partial q} \simeq \frac{f(q+\delta) - f(q-\delta)}{2\delta} \tag{17}$$

The accuracy and performance of the two will be further discussed and compared in the Section 5.

3.4 Exact and simplified solution

Another analysis was made introduced a third model called simplified model, where the second term of Equation (14) is equal to 0, so the dynamic equation is simplified in:

$$\frac{dp}{dt} = -[K]\boldsymbol{q} - C\dot{\boldsymbol{q}} + F[B(q)] \tag{18}$$

The goal of introducing this model is to compare with the full model solution to verify if the second term is relevant to the system motion and if it can or can not be disregarded. This was done with an initial displacement equivalent of the static response, (a particular case which will be further seen in sub-section 5) and the body was put in free vibration. The reason to choose a free vibration case is due to the fact that on Equation (14), the last term of generalized forces is equal to zero, which means that the observed term has a larger influence on the behavior of the structure motion.

4. NON-LINEAR REDUCED MODEL

The first step in order to begin the modal decomposition is to obtain the natural modes of the beam. This can be easily obtained by solving the associated eigenvalue problem for its static deformation.

$$\left([K] - [M_m(q)]\lambda\right)[\phi] = 0\,, \tag{19}$$

where $[\phi] = [\boldsymbol{\phi_1}, \boldsymbol{\phi_2}, \ldots, \boldsymbol{\phi_n}]$ is a square matrix with dimension n that contains the n eigenvectors that represent the structural displacement modes. λ is a square diagonal matrix with dimension n and the main diagonal contains the eigenvalues associated to each eigenvector.

The beam displacement can be seen as a combination of the different modes, but the first modes have a higher significance on the total beam dynamics, so by choosing a number of modes lower than the size of the problem discretization ($r < n$) it is possible to reduce the dimension of the system from n to r, applying the truncation method. The beam displacement can be approximated as

$$\boldsymbol{q} \simeq [\phi_r]\boldsymbol{\eta}\,, \tag{20}$$

where $[\phi_r] = [\boldsymbol{\phi_1}, \boldsymbol{\phi_2}, \ldots, \boldsymbol{\phi_r}]$ and $[\boldsymbol{\eta} = \eta_1, \eta_2, \ldots, \eta_r]$, with r < n. By substituting the reduced representation of the generalized coordinates of Equation 20 on Equation 8 that describes the global coordinates, the global coordinates can then be obtained using the reduced coordinates η.

$$\boldsymbol{h(\eta)^T} = [\phi_r]\{\boldsymbol{x(\eta)^T}, \boldsymbol{y(\eta)^T}\} \tag{21}$$

By substituting Equation (20) on the system Equations of Motion (13) and (14) the equations of motion for the reduced order system are obtained:

$$\frac{d\eta}{dt} = [M_{m,r}(\eta)]^{-1}\boldsymbol{p} \tag{22}$$

$$\frac{dp}{dt} = -[K_r]\boldsymbol{\eta} - \frac{\partial}{\partial \boldsymbol{\eta}}\left(\boldsymbol{p^T}[M_{m,r}(\eta)]^{-1}\boldsymbol{p}\right) - C\dot{\boldsymbol{\eta}} + F[B(\eta)] \tag{23}$$

where

$$[K_r] = [\phi_r]^T[K][\phi_r] \tag{24}$$

$$[M_{m,r}(\eta)] = J_{h,\eta}^T[M]J_{h,\eta} \tag{25}$$

$$[B_r(\eta)] = [\phi_r]^T J_{r,\eta}^T \left[-sin\left(\sum_{i=1}^{n}\phi_i\eta_i\right) \quad , \quad cos\left(\sum_{i=1}^{n}\phi_i\eta_i\right) \quad , \quad 0\right]^T \tag{26}$$

5. RESULTS

In this section, the equations of motion will be solved with the aid of *Matlab* and the results will be compared with the literature, evaluating the performance of the reduced-order model compared with the full one. Beyond that, a comparison between the methods of calculating the gyroscopic term, and a comparison between the full model and the simplified one, following the methodology presented in Section 3 beginning with the results of natural modes obtained with the approximation of calculated beam stiffness K_θ and K_ψ. These results are compared with the natural frequencies obtained with continuous beam models obtained via semi-analytical methods, which are well-known in the literature (REF). For displacements validation, a test case of the static response and a test case for the dynamical response, the analysis of using a numerical or exact gradient, and a full versus simplified model are made at first. All the test case displacements are compared with the results obtained by Brown (2003), with the intuit of validation.

5.1 Natural modes and frequencies

The natural modes were obtained solving the eigenvalue problem obtained using the eig function of $Matlab$. The torsional stiffness of the springs is calculated via Equation (6) and (7). The first nine modes with bending and torsion coupled ($d_0 \neq 0$) are compared to the same modes obtained with semi-analytical methods and validation between the natural frequencies of these modes are presented.

5.2 Non-linear bending motion

A more in-depth validation was made for the bending motion, given that it contains the non-linearities of the system. All following test cases use a second test case beam with properties listed below.

Table 1. Properties used for natural frequencies comparison beam

Length $L[m]$	16
Width $L[m]$	1
Mass/length $m_0[Kg/m]$	0.75
Moment of inertia $I_0[Kg.m^2]$	0.75
Center of mass offset $d_0[m]$	0.267
Stiffness $EI[Pa.m^2]$	2e4
Transversal Stiffness $GJ[Pa.m^2]$	1e3

Table 2. Validation of the first nine natural modes with coupled motion

	n = 16			n = 32		
Natural mode	Lumped-mass model frequency [rad/s]	Semi-analytical frequency [rad/s]	Error [%]	Lumped-mass model frequency [rad/s]	Semi-analytical frequency [rad/s]	Error [%]
First coupled	2.21	2.21	0.02	2.21	2.21	0.01
Second coupled	9.55	9.55	0.01	9.55	9.55	0.00
Third coupled	13.78	13.80	0.10	13.79	13.80	0.03
Fourth coupled	27.39	27.40	0.02	27.40	27.40	0.01
Fifth coupled	36.38	36.66	0.76	36.59	36.66	0.19
Sixth coupled	46.69	46.95	0.56	46.88	46.95	0.16
Seventh coupled	63.14	64.02	1.38	63.79	64.02	0.37
Eighth coupled	65.05	66.52	2.21	65.96	66.52	0.84
Ninth coupled	80.53	86.71	7.14	83.08	86.71	4.19

Table 3. Normalized CPU time and dimension comparison between full and reduced model static response

Solution	Dimension	CPU time
Full	20	1
Reduced, 2 modes	2	0.32
Reduced, 3 modes	3	0.36

Table 4. Properties used for non-linear bending comparison beam

Length $L[m]$	1
Width $L[m]$	0.05
Mass/length $m_0[Kg/m]$	0.2
Stiffness $EI[Pa.m^2]$	50

5.2.1 Static test case - Multiple points forces

The point vertical force at the beam tip has its intensity varied from $F1 = 0$ to $F1 = 150N$, and the load at the middle of the beam has constant intensity $F2 = -150N$. The generalized coordinate vector $\boldsymbol{q}$ of Equations (13) and (18), that describes the motion of the system was then calculated, Figure 4 shows the full and reduced models and Table 5 shows the results of computational performance.

5.2.2 Dynamical response

Before starting the dynamical test cases, a prior analysis felt necessary to be done. The first analysis refers to the use of a numerical or exact gradient to calculate the derivative term contained in Equation (14), and the second analysis creates an additional model called a simplified model that does not include this term. All simulations were executed using a variable step integrator $ode15s$ function. The simulations were run for $1s$, with a time-step of $0.005s$.

5.2.3 Computation of gyroscopic term

As said in Section 3.3the second term of Equation (14) that describes the full system dynamics contains a term that is impractical to calculate analytically due to the derivative of a matrix inversion in symbolical math, especially in the full model. To avoid that, a numerical calculation of the gradient was chosen and was verified comparing it to the exact solution calculated via numerical differentiation with the aid of $Adigator$ Patterson *et al.* (2013).

A pre-simulation was executed to obtain a representative vector q for the comparison of the gradients, in this case, the vector q chosen was the solution from the last time-step of the solution, where $t = 1s$, then the gradient was calculated

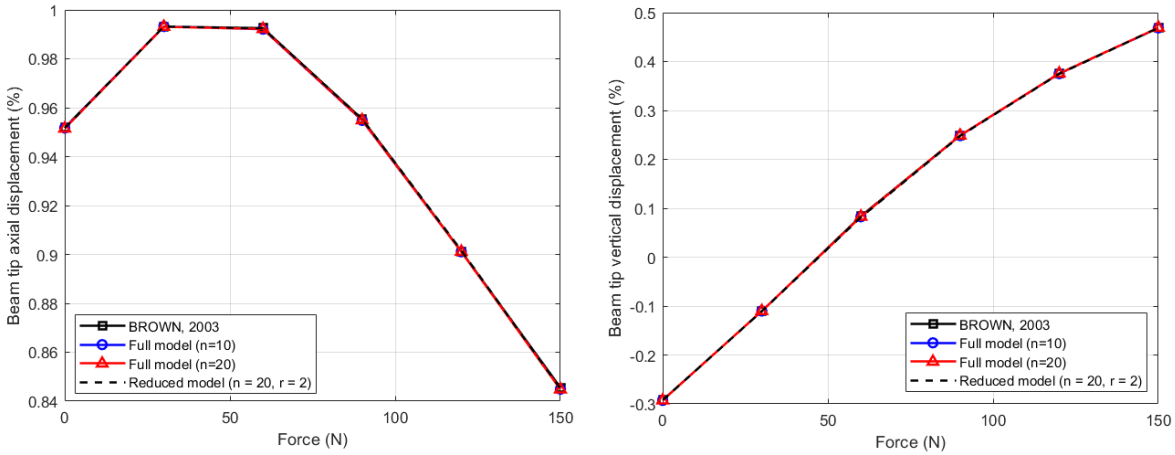

Figure 4. Static response of the full and reduced models for test case 2.

Table 5. Normalized CPU time and dimension comparison between full and reduced model static response

Solution	Dimension	CPU time
Full	10	1
Reduced, 2 modes	2	0.34
Reduced, 3 modes	3	0.32

numerically and exactly. For the numerical gradient calculation, a step of $h = 1 \times 10^{-6}$ was chosen. The result of the comparison is shown in Table 6 A sensitivity analysis was made, meaning that a further series of comparisons was

Table 6. Comparison between Exact and numerical gradient

Method	Mean absolute error	Mean Relative error	CPU time
Exact	0	0	1
Numerical	8.99×10^{-10}	1.26×10^{-8}	0.084

executed changing the parameters of the system, such as mass, stiffness, displacement, to verify if there is a case where the error between the numeric and the exact case amplifies. Despite that, it was verified that the error doesn't vary substantially, still remaining in a very small order of magnitude. It was safe to adopt for the remaining simulations the numerical gradient since it shows excellent accuracy with an enormous reduction in computation time.

5.2.4 Full and simplified model

In order to verify if the differential term of the dynamic equation is relevant, an analysis for the simplified and full numerical model was made. The test case chosen was the case of free vibration with the initial displacement condition of the static response of test case 1 (Vertical tip force of $F = 150N$). Due to computational limitation, the number of elements was reduced to $n = 10$ elements. Simulation is executed for both cases and the results are shown. A sensitivity

Table 7. Normalized CPU time and dimension comparison between full and simplified dynamic response

Solution	Dimension	CPU time
Full	10	1
Simplified	10	0.197

analysis was made and showed that the differential term increases with higher displacements, the simplified model has a small lag in comparison with the full model. In order to verify how this behavior propagates in time, another simulation was made increasing the total time from 1 s to 30 s. The values from the beam tip axial and vertical displacements were obtained and compared. Figure 5 shows the relative error between the simplified and full model. The displacements used for this case were already very high (over 60% of vertical tip displacement), Besides, in the following test cases, there will be a force acting on the structure, meaning that the effects of this term will be further minimized. In conclusion, the simplified model has a large computational gain over the full model and a small difference even in the extreme case, with a maximum value of the relative error of 4% that tends to decrease with long time simulations, as shown in Figure 5.

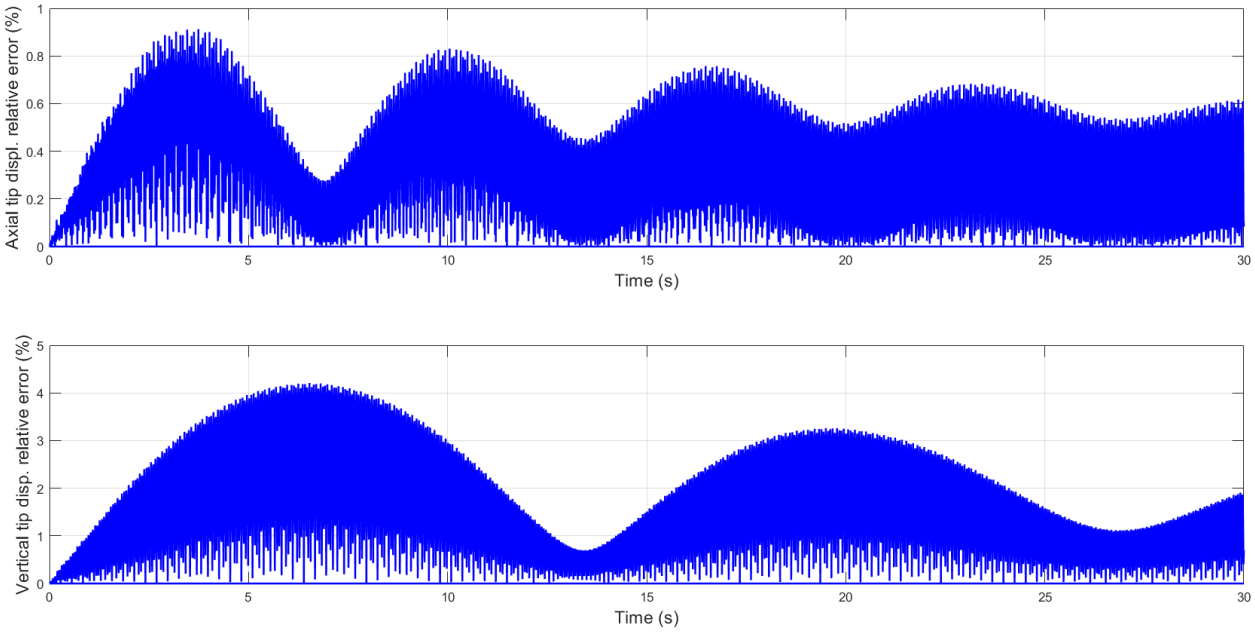

Figure 5. Beam axial and vertical relative error vs time

Due to shown evidence, the simplified model was chosen to represent the full numerical model in the further test cases to compare with the reduced-order model.

5.2.5 Dynamic test case - sinusoidal tip load

With the previous analysis made in the previous sections, it is now safe to compare the full and reduced model. With the same beam used in the static response test cases, it is now submitted to a sinusoidal force at the beam tip $F(t) = 10\sin(20t)$. The simulation is executed for the full and reduced-order models in order to find the values of $\boldsymbol{q}$ and $\boldsymbol{\eta}$ that satisfies Equations (14) and (23) respectively for each time step. As discussed in Section 5.2.4 the differential term of both equations is disregarded. The results are compared with Brown (2003) and are shown in Figure 6 and its computation performance in Table 8.

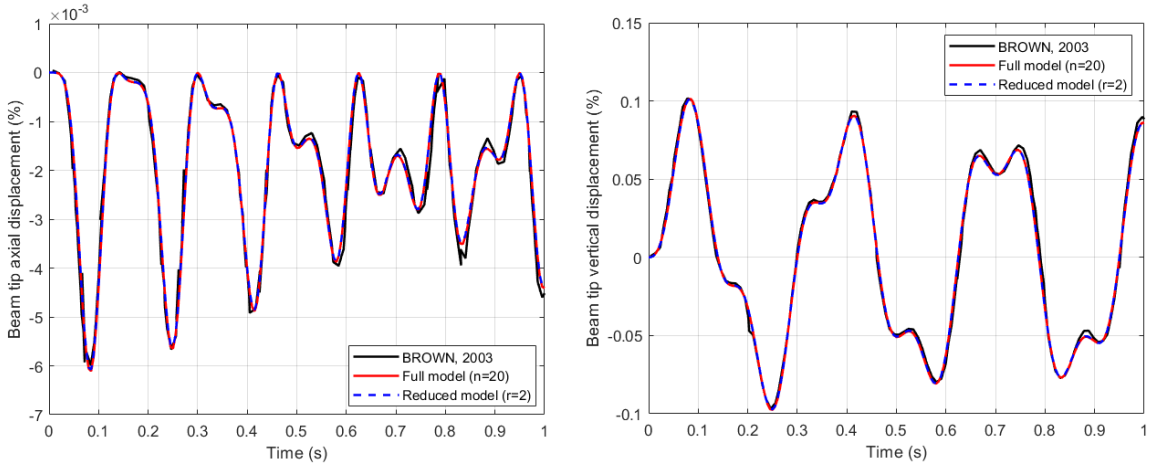

Figure 6. Comparison of the beam tip position at Test case 3.

Table 8. Normalized CPU time and dimension comparison between full and simplified dynamic response for Test case 3

Solution	Dimension	CPU time
Full	20	1
Reduced	2	0.146

6. CONCLUSIONS AND FURTHER WORK

As seen in the study made by Rempel *et al.* (2020) the number of elements is directly proportional to the accuracy of the approximation for the spring system stiffness, this has a beneficial synergy with the fact that a greater number of elements, also increases the advantages in computational time of the reduced system, although by calculating the value of each torsional spring stiffness, it was observed an excellent result for the static case even for the case with a low number of elements $(n = 10)$.

The reduced model gains more computational performance with lesser modes, however increasing the number of modes means that the approximation for the full model is more accurate, the static response is a good way to test the choice of a number of modes, larger displacements, and more complex forces or constraints requires a higher number of modes to make a good approximation of the full system, the goal is to choose the minimal number of modes that still represent with fidelity the full model.

The differential term of the dynamic equation discussed in Section 5.2.4was disregarded due to its low impact on long-time flight simulation of an aircraft, but if this structural model is used to couple on short-time systems, such as a control system, this is a point of attention.

By validating the results of the static and dynamic responses with the results obtained by Brown (2003), proved that an accurate approximation for obtaining torsional stiffness for the numerical model, based on a continual beam with stiffness EI, was obtained, even for the case with a low number of elements $(n = 10)$. It also achieved a good approximation for the system's natural frequencies, which allowed an accurate result for the dynamical responses as well.

The main objective of this study, which was to evaluate the computational gains of using a reduced model concluded that a reduction of CPU time of over 15 times was obtained, while still representing the behavior of the system very accurately, as shown in the test cases, which is a major success. The objectives of this study were concluded and a very surprising gain in computational performance and accuracy was observed in the results. For future studies, it is intended the use of a simple aerodynamic model for the inclusion of an aeroelastic analysis.

7. REFERENCES

Brown, E.L., 2003. *Integrated Strain Actuation In Aircraft With Highly Flexible Composite Wings*. Doctoral dissertation, Massachusetts Institute of Technology.

Hodges, D.H., 1990. "A mixed variational formulation based on exact intrinsic equations for dynamics of moving beams". *International Journal of Solids and Structures*, Vol. 26, No. 11, pp. 1253–1273. ISSN 0020-7683. doi: https://doi.org/10.1016/0020-7683(90)90060-9.

Medeiros, R., 2019. *Model Order Reduction for Aeroelastic Analysis of Very Flexible Aircraft*. Doctoral dissertation, University of Michigan.

Patil, M., 1999. *Nonlinear aeroelastic analysis, flight dynamics, and control of a complete aircraft*. Ph.D. thesis.

Patterson, M.A., Weinstein, M. and Rao, A.V., 2013. "An efficient overloaded method for computing derivatives of mathematical functions in matlab". *ACM Trans. Math. Softw.*, Vol. 39, No. 3, pp. 17:1–17:36. ISSN 0098-3500. doi:http://dx.doi.org/10.1145/2450153.2450155. URL `http://doi.acm.org/http://dx.doi.org/10.1145/2450153.2450155`.

Rempel, M.A., Ribeiro, F.L.C. and Moreira, F.J.O., 2020. "Lumped element multibody modeling approach for very flexible aircraft". In *Proceedings...* Ibero-Latin American Congress on Computational Methods in Engineering (CILAMCE).

Ribeiro, F.L.C., Paglione, P., da Silva, R.G.A. and de Sousa, M.S., 2012. "Aeroflex: a toolbox for studying the flight dynamics of highly flexible airplanes". In *Proceedings...* International Congress of Mechanical Engineering (CONEM).

Sandberg, H., 2019. "Introduction to model order reduction". URL `https://people.kth.se/ hsan/modred2019.htm`.

Schilders, W.H., van der Vorst, H.A. and Rommes, J., 2008. *Model Order Reduction: Theory, Research Aspects and Applications*. Springer, Eindhoven, The Netherlands, 1st edition.

Shearer, C.M., 2006. *Coupled nonlinear flight dynamics, aeroelasticity, and control of very flexible aircraft.* Doctoral dissertation, The University of Michigan, Ann Arbor.

Su, W., 2008. *Coupled Nonlinear Aeroelasticity And Flight Dynamics Of Fully Flexible Aircraft*. Doctoral dissertation, The University of Michigan, Ann Arbor.

Su, W. and Cesnik, C.E.S., 2014. "Strain-based analysis for geometrically nonlinear beams: A modal approach". *Journal of Aircraft*, Vol. 51, No. 3. URL `https://arc.aiaa.org/doi/10.2514/1.C032477`.

8. RESPONSIBILITY NOTICE

The authors are solely responsible for the printed material included in this paper.